

---

---

## REVIEW ARTICLE

---

---

# Magnetic Resonance Imaging for Rectal Submucosal Tumours

BTY Yuen<sup>1</sup>, EHY Hung<sup>1</sup>, CCM Cho<sup>1</sup>, SSF Hon<sup>2</sup>, AWH Chan<sup>3</sup>, HHL Chau<sup>1</sup>

<sup>1</sup>Department of Imaging and Interventional Radiology; <sup>2</sup>Division of Colorectal Surgery, Department of Surgery;

<sup>3</sup>Department of Anatomical and Cellular Pathology, Prince of Wales Hospital, The Chinese University of Hong Kong, Shatin, Hong Kong

### ABSTRACT

*A rectal submucosal tumour is defined as a mass-like protrusion in the rectum covered by normal mucosa. It comprises a variety of benign and malignant tumours that originate from the rectal wall or outside the rectum. Full characterisation by endoscopy or endoscopic biopsy is often difficult due to its deep location. Magnetic resonance imaging (MRI) can provide information about the origin, internal composition, and local extent of the tumour. Radiologists should be familiar with the types and MRI features of rectal submucosal tumours to facilitate accurate diagnosis and guide management.*

*Key Words:* Magnetic resonance imaging; Rectal neoplasms

## 中文摘要

### 直腸粘膜下腫瘤的磁共振成像

袁子祐、洪曉義、曹子文、韓溯飛、陳永鴻、周海倫

直腸黏膜下腫瘤的定義為由正常粘膜覆蓋的直腸質塊狀突起，其包含源自直腸壁或直腸外的各種良性和惡性腫瘤。由於其位置較深，通過內窺鏡檢查或內窺鏡活檢進行全面特徵描述通常是困難的。磁共振成像（MRI）能提供關於病變的起源、內部組成和局部範圍的信息。放射科醫師應熟悉直腸黏膜下腫瘤的類型和MRI特徵，以便進行準確的診斷和指導治療。

### INTRODUCTION

A rectal submucosal tumour is defined as a mass-like protrusion in the rectum covered by normal mucosa. It comprises a variety of benign and malignant tumours of intramural or extramural origin. Those with an intramural origin include neuroendocrine tumour, gastrointestinal stromal tumour (GIST), schwannoma,

melanoma, and metastatic spread to the rectum. Those with an extramural origin include deep endometriosis, tailgut cyst, and direct invasion by extra-colonic tumour. Imaging features of these tumours are shown in the Table.

Conventional colonoscopy can identify submucosal

---

*Correspondence:* Dr BTY Yuen, Department of Imaging and Interventional Radiology, Prince of Wales Hospital, The Chinese University of Hong Kong, Shatin, Hong Kong.  
Email: yty1120@hotmail.com

Submitted: 4 Nov 2017; Accepted: 4 Dec 2017.

Disclosure of Conflicts of Interest: All authors have disclosed no conflicts of interest.

**Table.** Key imaging features of rectal submucosal tumours.

Tumour	Imaging feature
Intramural origin	
Neuroendocrine tumour	Mid-rectum; small superficial well-circumscribed submucosal mass causing endoluminal bulge; no significant exophytic component; intense contrast enhancement
Gastrointestinal stromal tumour	Well-circumscribed predominant exophytic mass; absence of invasion of adjacent organs and lymphadenopathy despite large tumour size
Schwannoma	Well-circumscribed mass; T2 hyperintensity representing cystic or myxoid component; commonly accompanied by enlarged reactive lymph nodes in the mesorectum due to lymphoid cuffing around tumour
Melanoma	Anorectal junction; large polypoidal mass with local invasion; T1 hyperintensity if melanocytic; frequently associated with nodal metastases
Metastatic spread to the rectum	Known primary malignancy; features similar to primary tumour; located in the upper rectum in contact with the peritoneum if spread by serosal deposits
Extramural origin	
Endometriosis	Anterior rectal wall; infiltrative T2-hypointense fibrotic tumour; mushroom cap sign; punctate T1-hyperintense foci indicating subacute blood
Tailgut cyst	Retrorectal; multilocular cystic mass with multiple small cysts clustering adjacent to a main cyst; different signal intensities of locules; rim enhancement

tumours but not their characteristics. Transrectal ultrasonography can localise the specific mural layer of origin, but has limitations in the evaluation of large tumours, high rectal tumours, relationship of the tumour with the anal sphincter complex, and other pelvic organs. The diagnostic accuracy of transrectal ultrasonography-guided fine-needle aspiration / biopsy for rectal subepithelial tumours has been reported to be only 50%.<sup>1</sup>

Magnetic resonance imaging (MRI) has a high soft-tissue contrast and multiplanar capability and enables discrimination of different layers of the rectal wall and evaluation of the origin and internal composition of rectal submucosal tumours. MRI is the investigative tool of choice for the complex anatomy of the pelvis and the relationship of tumours with the pelvic floor, sphincter complex, and adjacent organs to facilitate surgical planning.

This review aimed to highlight the common types of rectal submucosal tumours encountered in clinical practice and their MRI features in order to facilitate accurate diagnosis and guide management.

## MAGNET RESONANCE IMAGING PROTOCOL

An MRI protocol to evaluate rectal submucosal tumours includes axial T1-weighted and T2-weighted turbo spin-echo (TSE) imaging of the pelvis, T1-weighted 3D gradient-echo fat-suppressed imaging of the pelvis, sagittal and oblique axial 3-mm high-resolution T2-weighted TSE sequences of the rectum, coronal 3-mm

high-resolution T2-weighted TSE sequences parallel to the anal canal for low-lying tumours, axial T1-weighted 3D gradient-echo fat-suppressed imaging of the pelvis following intravenous injection of gadolinium-based contrast material, diffusion-weighted imaging of the pelvis with b values of 0, 500, and 1000 sec/mm<sup>2</sup>, and reconstruction of an apparent diffusion coefficient map. A phased array coil is used; an intravenous anti-spasmodic is routinely administered unless contraindicated. Prior rectal preparation is not required.

### Intramural Origin

#### *Neuroendocrine Tumour*

Approximately 34% of neuroendocrine tumours of the gastrointestinal tract (previously known as carcinoid tumours) occur in the rectum, mostly the mid-rectum.<sup>2,3</sup> They develop from the muscularis mucosa or submucosal layer and are commonly circumscribed.<sup>2,4</sup> Approximately 79% of such tumours are <1 cm and only 5% are >2 cm. Most patients are asymptomatic and tumour detection is often incidental during routine endoscopy for unrelated symptoms.

Rectal neuroendocrine tumours have a good prognosis. Tumour size and micro-invasiveness are the most important prognostic factors.<sup>4</sup> Risk factors for metastatic disease include tumour size, muscularis propria invasion, proliferative index, and lymphovascular and perineural invasion.<sup>3</sup> Patients with a larger tumour are often referred for further imaging before excision. Patients with unfavourable histology after excision are referred for MRI to exclude metastasis in the mesorectum.

Due to its origin in the superficial layers of the rectal wall, rectal neuroendocrine tumours typically appear as a small superficial submucosal mass causing endoluminal bulging but without a significant exophytic component. The tumour is usually isointense on T1-weighted images and hyperintense on T2-weighted images, with moderate-to-intense contrast enhancement (Figure 1).<sup>4-6</sup> In pancreatic neuroendocrine tumours, lower apparent diffusion coefficient values correlate with higher histological grades.<sup>7,8</sup> Nonetheless, such correlation has not been investigated for primary gastrointestinal neuroendocrine tumours.

**Gastrointestinal Stromal Tumour**

GIST is the most common mesenchymal neoplasm of the gastrointestinal tract. It is defined by the expression of KIT (CD117), a tyrosine kinase growth factor receptor, that distinguishes GISTs from other mesenchymal neoplasms (such as leiomyoma, leiomyosarcoma, schwannoma, and neurofibroma) and determines the appropriateness of KIT-inhibitor therapy.<sup>9</sup> The most frequent sites of GIST are the stomach (60-70%) and small intestine (20-25%); only 5% of GISTs arise in the rectum.<sup>4</sup>

Most GISTs arise within the muscularis propria of

the intestinal wall and thus have an exophytic growth pattern and manifest as a dominant mass outside the organ of origin without invasion into adjacent organs (Figure 2).<sup>9</sup> Dominant intramural and intraluminal masses are less common radiological manifestations.<sup>9</sup> On MRI, GISTs are usually seen as an eccentric mural mass with well-circumscribed margins. Compared with muscle, GISTs show T1 hypointensity and mild T2 hyperintensity, with moderate heterogeneous gadolinium contrast enhancement. Mucosal ulceration may be seen. Restricted diffusion is a common feature due to the high cellularity of the tumour (Figure 3). There is a negative linear correlation between the mean apparent diffusion coefficient values and the malignancy risk of GISTs.<sup>10</sup> The prevalence of intra-tumoural cystic change that indicates tumour necrosis is higher in the moderate-to-high risk group than in the very low-to-low risk group.<sup>10</sup> Higher-risk GISTs may metastasise to the liver and peritoneum, but lymph node metastasis is rare (<3%).<sup>11</sup> Hence, lymphadenopathy in the mesorectum is not a common feature of rectal GIST.

**Schwannoma**

In the gastrointestinal tract, schwannomas mostly occur in the oesophagus and stomach, followed by the small intestine and appendix. Schwannomas of the colon

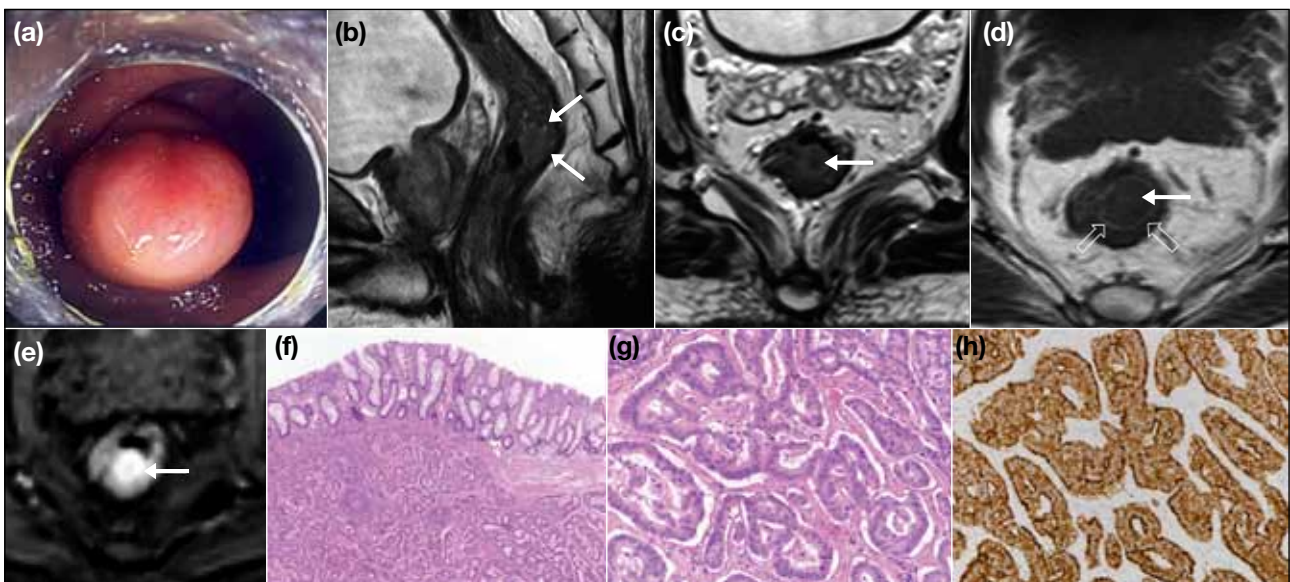


**Figure 1.** Neuroendocrine tumour: (a) a submucosal mass with a tinge of yellowish colouration in the overlying mucosa typical of rectal neuroendocrine tumour. (b) Sagittal T2-weighted, (c) axial T2-weighted, (d) axial T1-weighted, (e) and post-contrast T1-weighted, fat-suppressed images showing a small endoluminal tumour (arrows) in the mid-rectum with intense homogeneous contrast enhancement. The hyperintense submucosa (open arrows) is preserved in keeping with a superficial submucosal tumour without involvement of muscularis propria. Histology of the submucosal tumour showing (f) acini and nests of uniform tumour cells (H&E, x 20), (g) presence of minimal nuclear atypia and absence of mitosis (H&E, x 200), and (h) cells that are diffusely immunoreactive to neuroendocrine marker (synaptophysin, x 200).

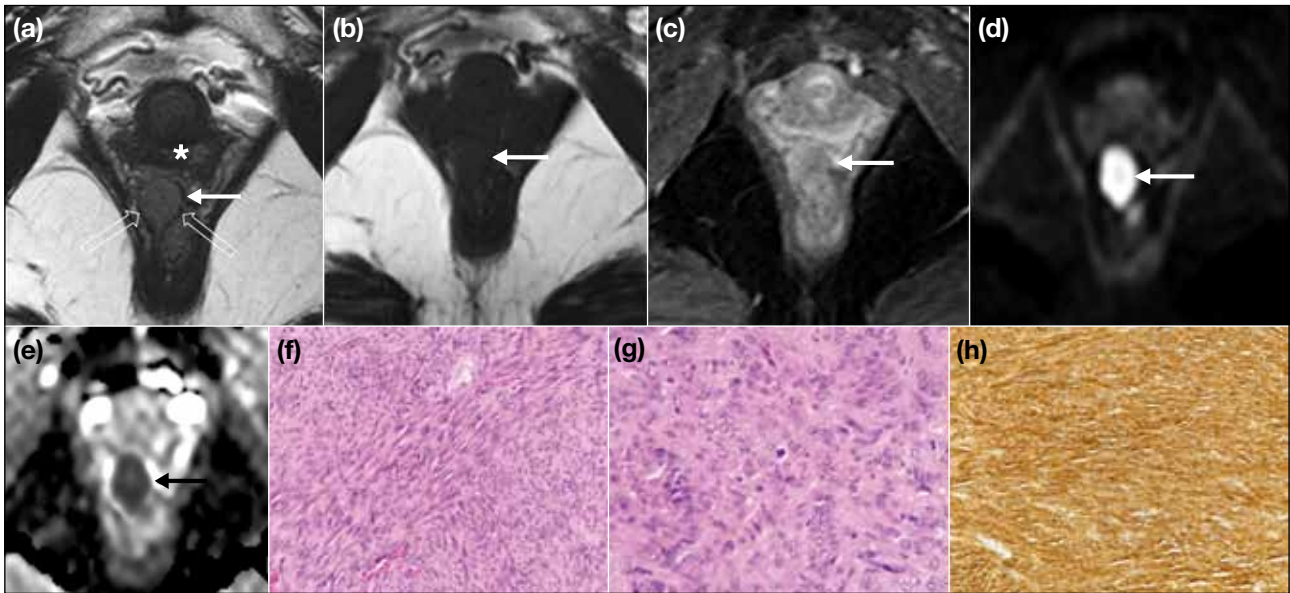


**Figure 2.** Gastrointestinal stromal tumour: axial (a) T2-weighted, (b) T1-weighted, and (c) post-contrast T1-weighted, fat-suppressed images showing an exophytic mass (arrows) arising from the muscularis propria (open arrows) of the low rectum and indenting the posterior wall of the vagina (asterisk), with an intact layer of muscularis propria (open arrows) around the tumour. The tumour shows homogeneous mild T2 hyperintensity, T1 hypointensity, and moderate contrast enhancement. (d) Axial b-1000 diffusion-weighted imaging and (e) apparent diffusion coefficient map showing marked restricted diffusion (arrows) due to high-tumour cellularity. Histology of the tumour showing (f) fascicles of spindle cells with mild cytological atypia and moderate amount of amphophilic cytoplasm (H&E, x 100), (g) a mitotic figure in a tumour cell (H&E, x 400), and (h) cells that are diffusely immunoreactive to CD117/c-kit (CD117/c-kit, x 100).

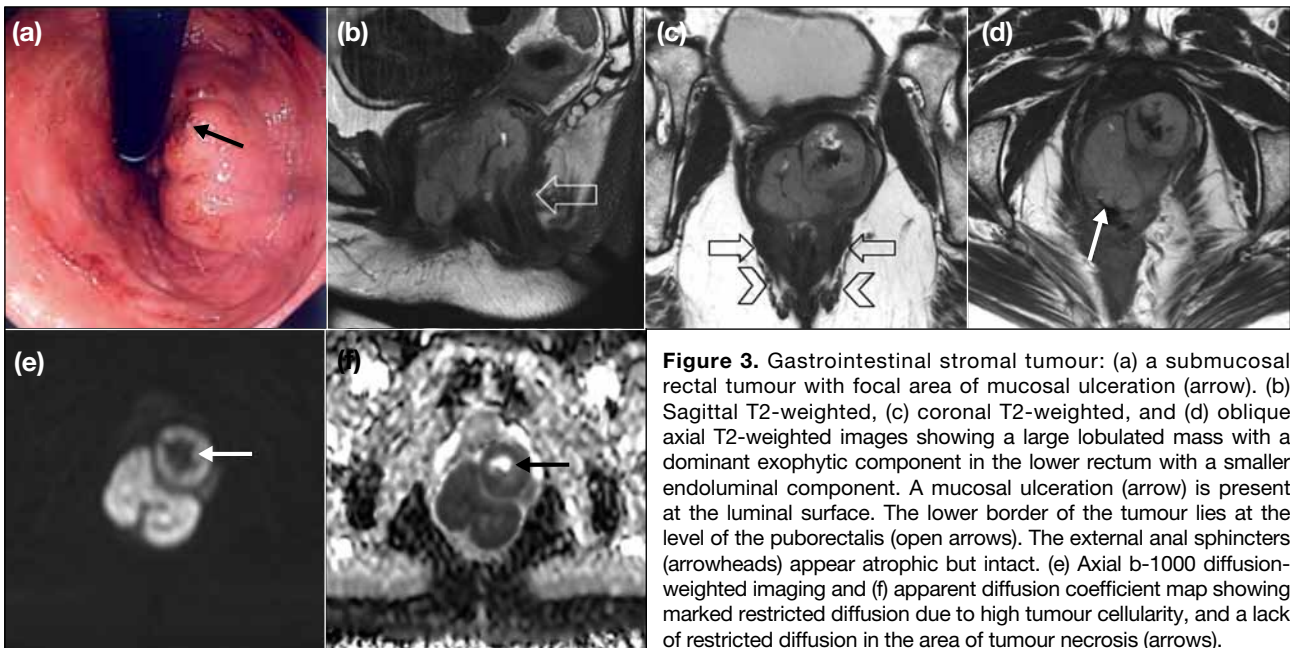


**Figure 3.** Gastrointestinal stromal tumour: (a) a submucosal rectal tumour with focal area of mucosal ulceration (arrow). (b) Sagittal T2-weighted, (c) coronal T2-weighted, and (d) oblique axial T2-weighted images showing a large lobulated mass with a dominant exophytic component in the lower rectum with a smaller endoluminal component. A mucosal ulceration (arrow) is present at the luminal surface. The lower border of the tumour lies at the level of the puborectalis (open arrows). The external anal sphincters (arrowheads) appear atrophic but intact. (e) Axial b-1000 diffusion-weighted imaging and (f) apparent diffusion coefficient map showing marked restricted diffusion due to high tumour cellularity, and a lack of restricted diffusion in the area of tumour necrosis (arrows).

and rectum are rare.<sup>4</sup> The ratio of GIST to colonic schwannoma has been reported to be 8-100:1.<sup>12</sup>

On MRI, schwannomas are typically a well-

circumscribed submucosal mass with T2 hyperintensity representing the myxoid component. Multiple schwannomas may be encountered. Contrast enhancement can be heterogeneous if the tumour is

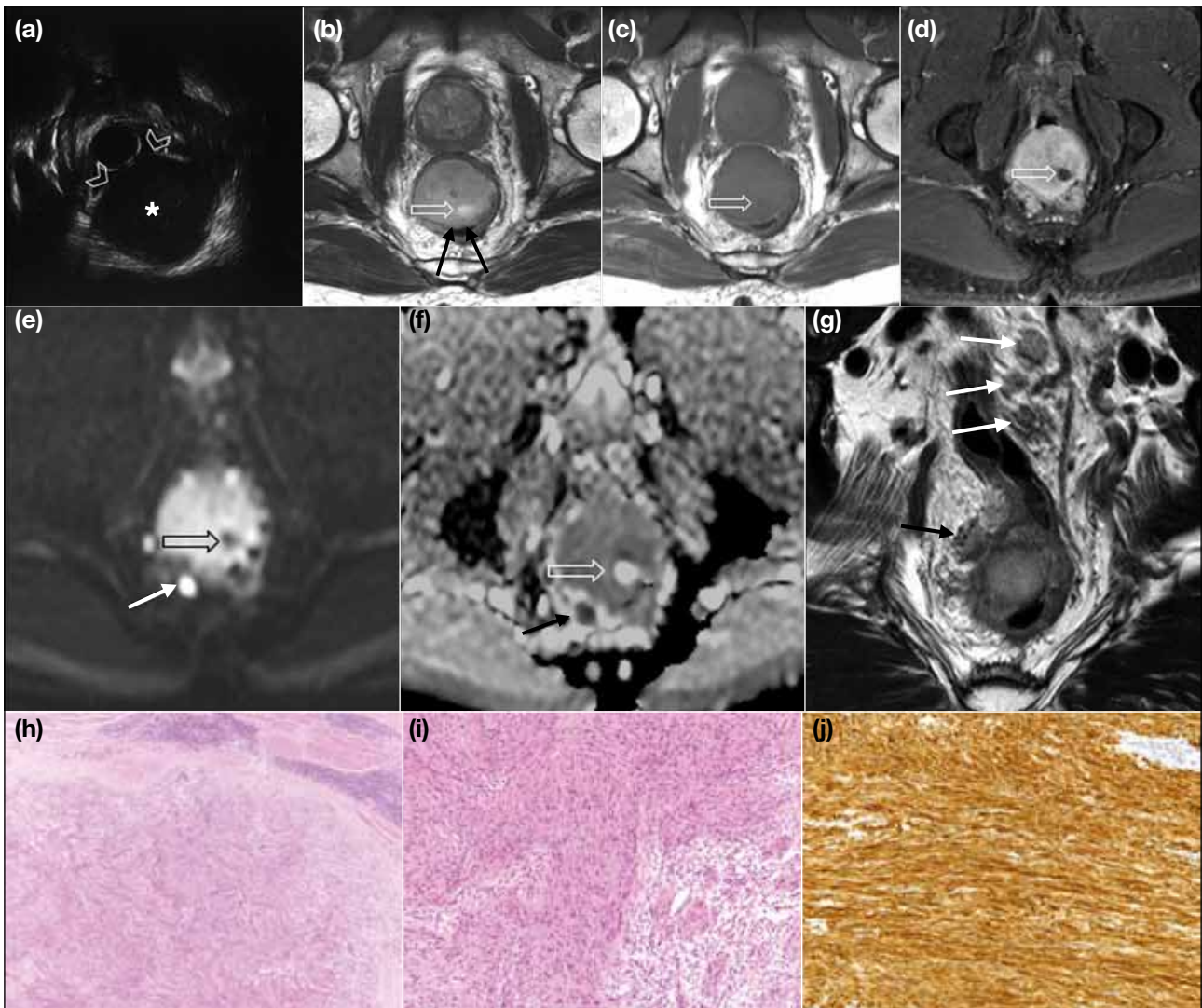


**Figure 4.** Schwannoma: (a) endoscopic ultrasonography showing a well-circumscribed hypoechoic submucosal mass (asterisk) in the superficial layer of the rectal wall, and an intact mucosa (arrowheads) overlying the tumour. (b) Axial T2-weighted, (c) axial T1-weighted, and (d) post-contrast T1-weighted, fat-suppressed images showing a submucosal tumour covered by normal mucosa (arrows) in the lower rectum. The area of high T2 intensity (open arrows) represents the myxoid component. (e) Axial b-1000 diffusion-weighted imaging and (f) apparent diffusion coefficient map showing moderate restricted diffusion of the tumour and shine-through effect of the myxoid component (open arrows), and restricted diffusion of a mesorectal lymph node (arrows). (g) Coronal T2-weighted image showing multiple enlarged mesorectal lymph nodes (arrows) that are pathologically benign. Nodal enlargement is common in rectal schwannoma due to lymphoid cuff around the tumour. Histology of the tumour showing (h) non-encapsulated, scattered lymphoid tissue with a rim (H&E, x 20), (i) spindle cells in alternating hypercellular and hypocellular growth patterns (H&E, x 100), and (j) cells that are diffusely immunoreactive to S100 (S100, x 100).

large and the myxoid component does not enhance. Restricted diffusion reflects its high cellularity. Radiological features of schwannoma considerably overlap those of other mesenchymal tumours such as GIST that is more common in the rectum. Nonetheless, GISTs are usually larger than schwannomas (mean, 6.3 cm vs. 2.4 cm) and seldom develop nodal metastases.<sup>12</sup>

In contrast, schwannomas are exclusively accompanied by enlarged lymph nodes; the underlying reason might be the presence of lymphoid cuffing around the tumour.<sup>12</sup> Schwannoma is a differential diagnosis of rectal submucosal tumours when a submucosal mass is detected with enlarged lymph nodes in the mesorectum (Figure 4).<sup>12</sup>

**Melanoma**

Melanoma is a highly aggressive malignant tumour that rarely arises in the anorectum.<sup>13</sup> Melanomas originate from melanocytes that are cells derived from the embryological neural crest. During foetal development, melanocytes migrate throughout the body, primarily to the skin, but a small number also reside in the eyes (retina and uveal tract) and mucosal surfaces. Cutaneous melanomas account for >90% of all melanomas and mucosal melanomas for <2%.<sup>14</sup> In the anorectal region, a primary melanoma arises from melanocytes at the anal transitional zone between columnar epithelium and squamous epithelium, and progresses upwards from the submucosa towards the rectum.<sup>15</sup> Therefore, most tumours arise at or slightly above the dentate line and rarely in the rectal location. Anorectal melanoma can present as a mucosal or submucosal mass. In the early stage of disease, they are often misdiagnosed as thrombosed haemorrhoids or skin tag. In most cases, they manifest late as bulky intraluminal masses without causing obstruction and are associated with perirectal infiltration and nodal metastases.<sup>16</sup>

Melanoma cells may carry melanin pigment that

shortens the T1 relaxation time due to the paramagnetic element. Melanoma also has a propensity to bleed. These account for the classic T1 hyperintensity in <50% of melanomas. Nonetheless, T1 hyperintensity is not shown in melanomas with <10% melanin-containing cells, and up to one-third of anorectal melanomas are amelanocytic (Figure 5). On T2-weighted images, melanomas are typically hypointense but may contain mixed signal intensity. These are hypercellular and hypervascular tumours, and hence restricted diffusion and contrast enhancement are typically present.<sup>16,17</sup> Regional nodal metastases occur in about half of the cases at diagnosis.<sup>18,19</sup>

The prognosis of anorectal melanoma is poor. Surgery remains the standard treatment, whereas systemic therapy is often palliative.<sup>18</sup> Due to its almost invariable involvement of the anorectal junction and high chance of local infiltration, MRI is important in the evaluation of local extent and operability.

**Metastatic Spread to the Rectum**

Metastasis from a distant primary tumour to the rectum is extremely rare. It can occur by direct invasion of

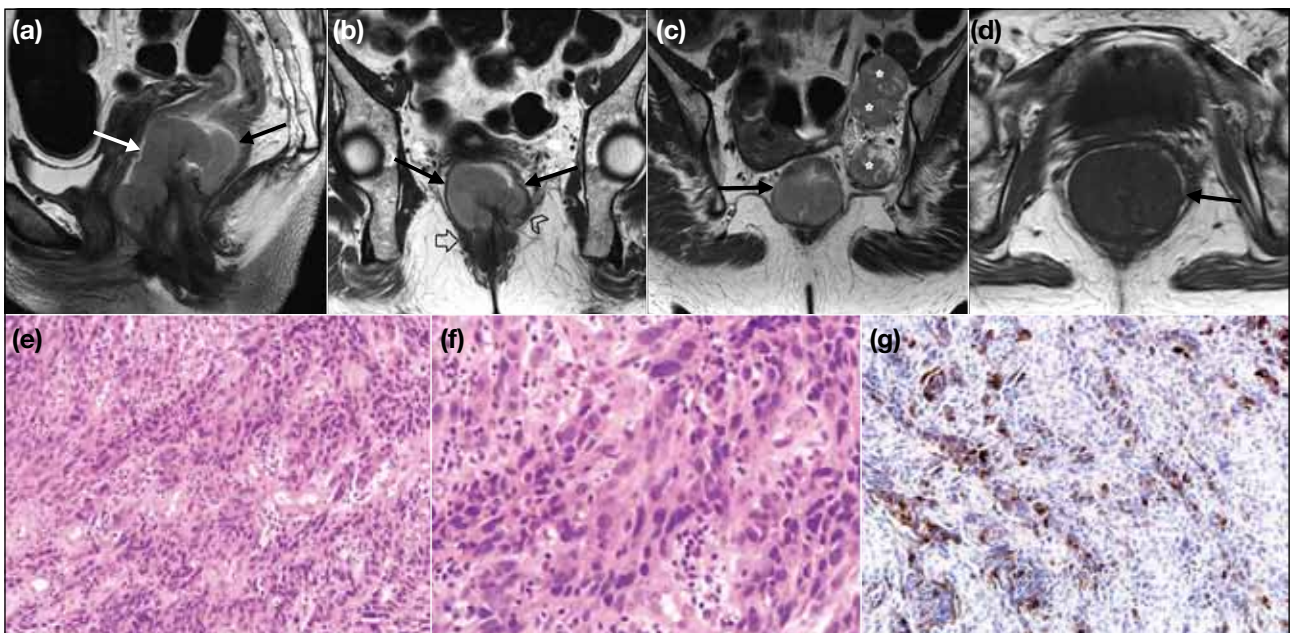


**Figure 5.** Melanoma: (a) sagittal T2-weighted, (b) coronal T2-weighted, and (c) axial T1-weighted images showing a large polypoidal endoluminal mass (arrows) in the lower rectum arising at the level of the puborectalis (open arrow). The tumour invades the left levator ani muscle, with multiple large necrotic left pelvic sidewall nodal metastases (asterisks). (d) The tumour is hypointense on T1-weighted image because of scanty melanin-containing cells. Histology of the tumour showing (e) loose sheets of pleomorphic epithelioid to plump spindle cells, admixed with scattered inflammatory cells (H&E, x 100), (f) markedly pleomorphic cells with enlarged nuclei and prominent nucleoli (H&E, x 400), and (g) cells that are focally immunoreactive to melanocytic marker (Melan-A, x 100).

metastatic deposits in the pelvis such as by lymph nodes, serosal metastatic deposits in peritoneal carcinomatosis, or via haematogenous spread. Nearly all malignancies have the potential to metastasise to the subperitoneal or peritoneal space, most commonly gastrointestinal and ovarian primary carcinomas.<sup>20</sup> Serosal metastatic deposits may be found in the upper and mid rectum that is in contact with the anterior peritoneal reflection (Figure 6). In a multi-centre study of approximately 10,000 patients with malignant colorectal tumours, only 35 patients (0.3%) had metastases through haematogenous spread to the colon or rectum from distant primary tumours, with the breast being the most common primary site, followed by melanoma, lung, bone and soft-tissue sarcoma, and kidney.<sup>21</sup>

Metastatic spread to the rectum indicates a late-stage of the disease and a poor prognosis, but it may occur up to 10 years after diagnosis of the primary tumour, particularly in patients with primary renal cell carcinoma.<sup>22</sup> MRI allows evaluation of the local extent and scrutiny for other metastatic involvement in the pelvis. MRI features of rectal metastasis are similar to

those of primary tumours. Radiologists should be aware of this, especially in patients with a history of primary malignancies.

### Extramural Origin

#### Endometriosis

Endometriosis is defined as the presence of functional endometrial glands and stroma outside the uterine cavity. Deep pelvic endometriosis, also known as deep-infiltrating endometriosis, is defined as subperitoneal invasion by endometriotic tumour that exceeds 5 mm.<sup>23</sup> It can affect various fibromuscular pelvic structures, with the recto-vaginal septum and uterosacral ligaments being most common (69.2%), followed by the alimentary tract (9.9%), with the rectosigmoid colon being the most common bowel segment.<sup>23</sup>

Unlike superficial endometriosis or ovarian endometriosis, deep pelvic endometriosis is often associated with pelvic pain, dyspareunia, and infertility. It is a differential diagnosis of rectal submucosal tumour if a submucosal rectal mass is seen in a symptomatic premenopausal woman.<sup>4</sup>

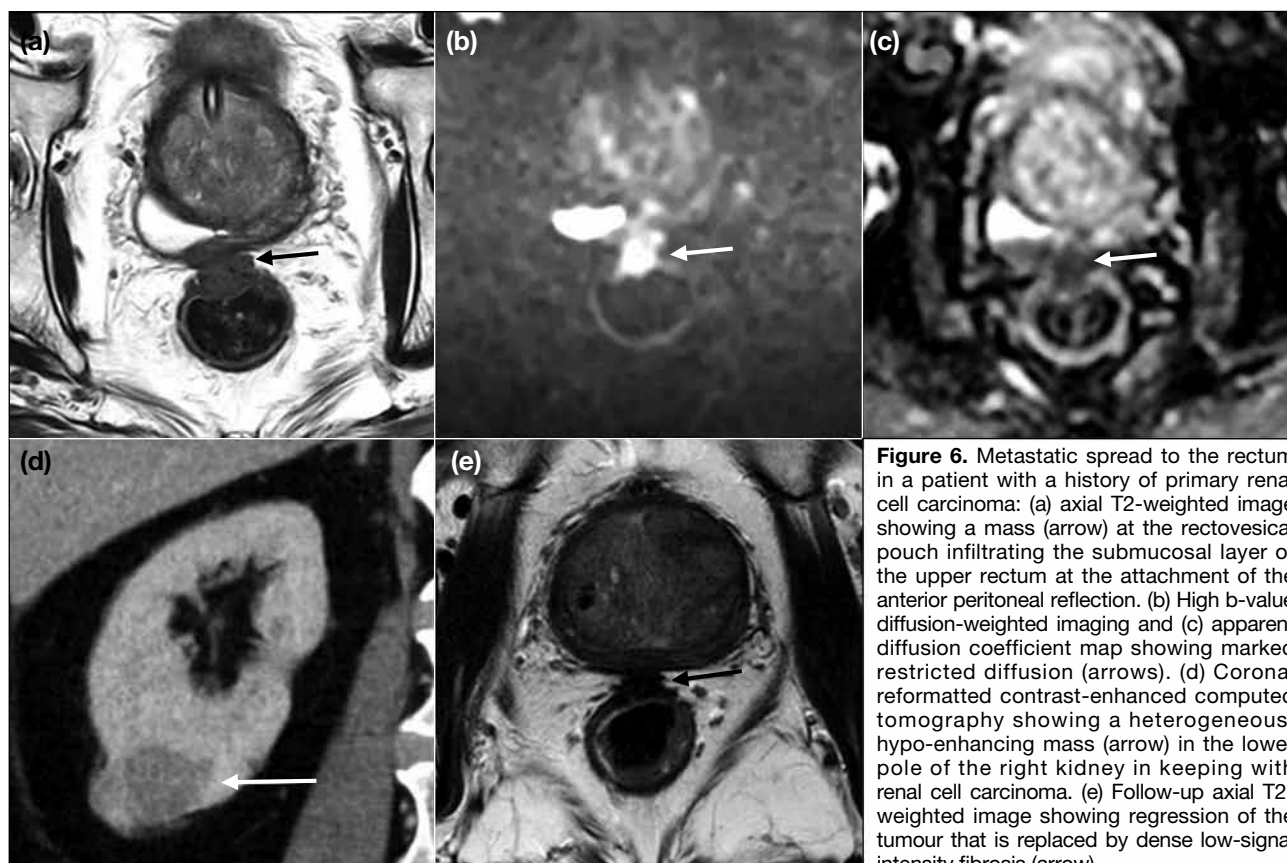


**Figure 6.** Metastatic spread to the rectum in a patient with a history of primary renal cell carcinoma: (a) axial T2-weighted image showing a mass (arrow) at the rectovesical pouch infiltrating the submucosal layer of the upper rectum at the attachment of the anterior peritoneal reflection. (b) High b-value diffusion-weighted imaging and (c) apparent diffusion coefficient map showing marked restricted diffusion (arrows). (d) Coronal reformatted contrast-enhanced computed tomography showing a heterogeneous, hypo-enhancing mass (arrow) in the lower pole of the right kidney in keeping with renal cell carcinoma. (e) Follow-up axial T2-weighted image showing regression of the tumour that is replaced by dense low-signal intensity fibrosis (arrow).

Endometriotic tumour manifests as an irregular, infiltrative, T2-hypointense mass with discrete fibrotic reaction due to chronic repetitive bleeding and scarring. It often penetrates the muscularis propria and invades the submucosa involving at least 40% of the circumference in the anterior rectal wall. On T2-weighted images, a ‘mushroom cap’ sign is indicative of solid invasive endometriosis of the rectosigmoid colon.<sup>24</sup> The low-signal intensity of the mushroom base is attributed to hypertrophy and fibrosis of the muscularis propria, whereas the high-signal intensity of the cap represents the mucosa and submucosa that are displaced into the bowel lumen. Small internal cystic foci represent ectopic endometrial glands, but their visualisation depends on location and the patient’s immune response. Hyperintensity on T1-weighted, fat-suppressed images indicates subacute blood and is specific for endometriosis (Figure 7).<sup>25</sup> Such finding is less common in deep pelvic endometriosis because the surrounding fibrosis and muscular hypertrophy minimise cyclical bleeding in the ectopic endometrial glands. The degree of contrast enhancement is variable and heterogeneous, depending on the glandular and fibrotic component of the tumour.

**Tailgut Cyst**

Tailgut cyst (retrorectal cystic hamartoma) is a rare developmental tumour thought to arise from vestiges of an embryonic hindgut and is found in the retrorectal (presacral) space.<sup>26</sup> It is more commonly found in middle-aged women.<sup>26</sup> Tailgut cyst usually presents as a multilocular cystic tumour with multiple small cysts clustering adjacent to a main cyst, giving rise

to a honeycomb appearance. It is typically located in the retrorectal space above the pelvic floor although extension through the levator muscle to the ischioanal fossa may occur.<sup>27,28</sup> It adheres to the sacrum and rectum but does not communicate with the rectal lumen. Erosion of the sacrococcygeal bone may occur.<sup>28</sup> The signal intensities on T1- and T2-weighted images vary according to the protein, mucin, and blood content of the cysts. In most tumours, the dominant cysts are hyperintense on T1-weighted images, with reference to the pelvic musculature (Figure 8). Infection, fistulation, recurrence after excision, and malignant degeneration are potential complications. The presence of enhancing solid components should raise the suspicion of malignant transformation although this is rare.<sup>4,26,28,29</sup> Differential diagnoses of a retrorectal cystic mass include mature cystic teratoma, epidermoid cyst, dermoid cyst, rectal duplication cyst, and anterior sacral meningocele (that are usually unilocular), as well as tailgut cyst and cystic lymphangioma (that are usually multilocular); there is substantial overlap among these entities.<sup>4,26</sup>

**Direct Rectal Invasion by Extra-colonic Pelvic Tumour**

Primary tumours arising from other pelvic organs (such as the uterus, ovary, or prostate) may invade the rectum. On endoscopy, it is difficult to differentiate among extrinsic tumours invading the rectum, extrinsic tumours indenting but not invading the rectal wall, and primary rectal intramural tumours. The primary role of MRI in this entity is to identify the primary tumour site (Figures 9 and 10).

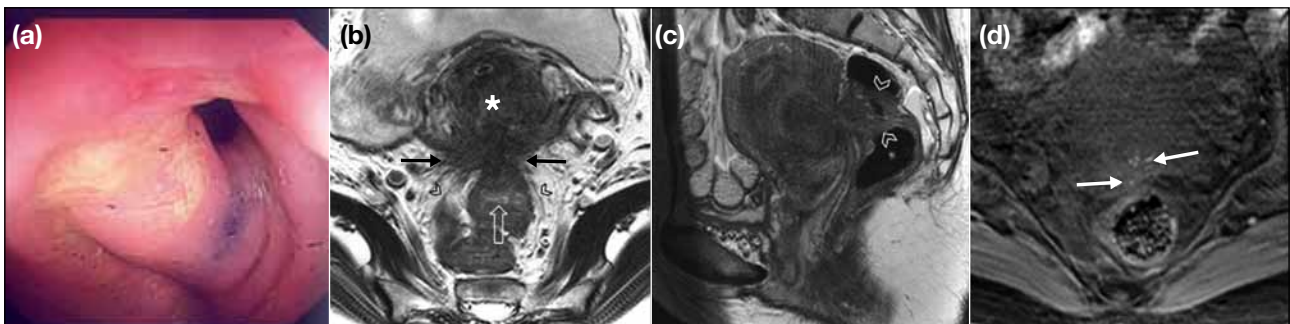


**Figure 7.** Deep endometriosis: (a) a mass-like protrusion into the rectal lumen covered by normal mucosa which is otherwise non-specific. (b) Axial T2-weighted image showing an infiltrative hypointense tumour (arrows) in the pouch of Douglas invading the anterior wall of the rectum (open arrow) and infiltrating the myometrium (asterisk). The markedly low T2 signal (similar to that of pelvic muscle) and fibrotic reaction are due to repetitive bleeding and scarring. Bilateral uterosacral ligaments are thickening (arrowheads). (c) Sagittal T2-weighted image showing the endoluminal bulging (arrowheads) into the rectal lumen as the ‘mushroom cap’ sign. (d) Axial T1-weighted, fat-suppressed image showing multiple punctate foci of T1 hyperintensity (arrows) indicating subacute blood.



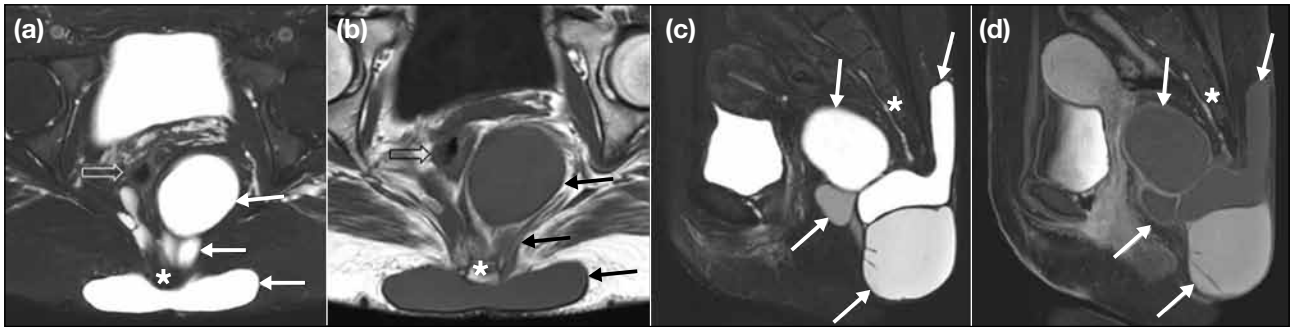


**Figure 8.** Tailgut cyst: axial (a) T2-weighted, fat-suppressed and (b) T1-weighted images showing a multiloculated cystic mass (arrows) in the retrorectal region and extending posteriorly to the coccyx (asterisks) to the subcutaneous layer. The rectum (open arrows) is displaced anteriorly. Sagittal (c) T2-weighted, fat-suppressed and (d) post-contrast T1-weighted, fat-suppressed images showing the different intensities of the multiple locules due to different contents (arrows). The wall of the locules shows rim enhancement despite no solid component.

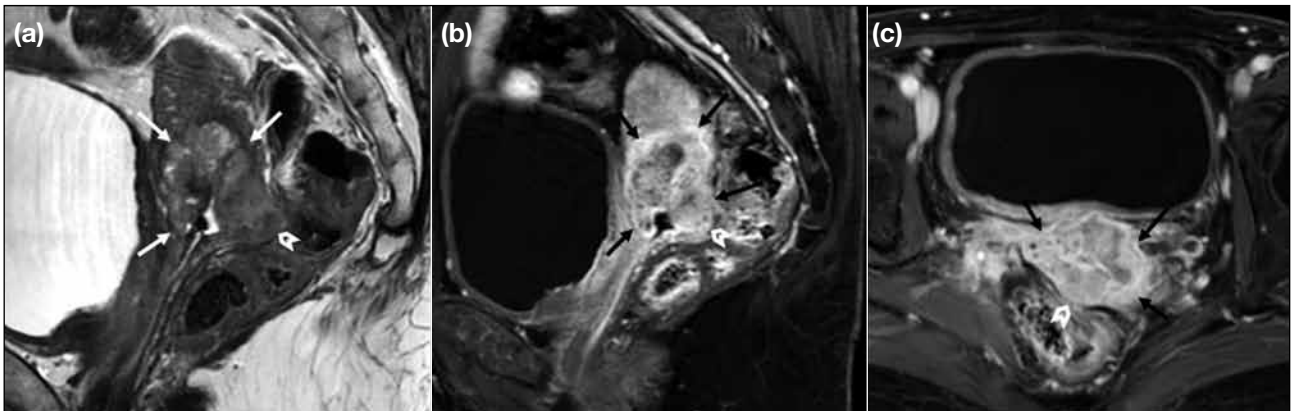


**Figure 9.** Carcinoma of the cervix invading the rectum: (a) sagittal T2-weighted, (b) sagittal post-contrast T1-weighted fat-suppressed, and (c) axial post-contrast T1-weighted fat-suppressed images showing an irregular heterogeneous mass (arrows) in the cervix invading the outer rectal wall (arrowheads) and the corpus.

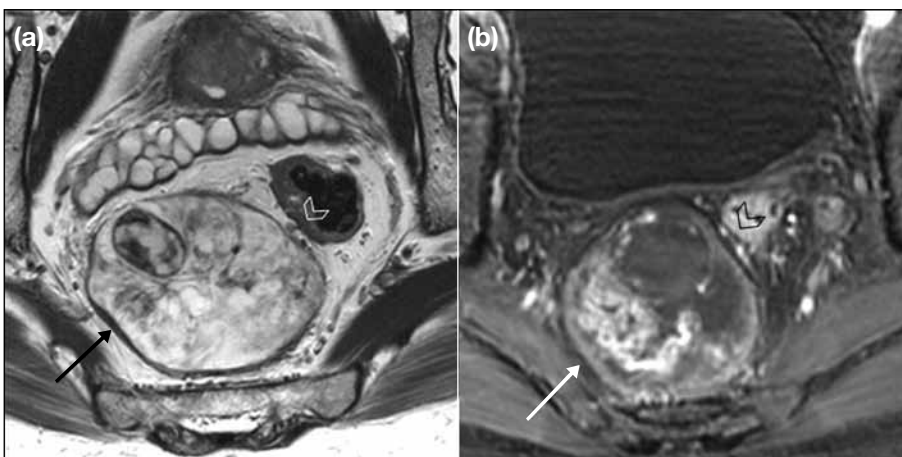


**Figure 10.** Peri-rectal schwannoma compressing the rectum: (a) axial T2-weighted and (b) axial post-contrast T1-weighted, fat-suppressed images showing a large heterogeneous T2 hyperintense mass (arrows) representing an old schwannoma in the mesorectum with mass effect on the posterior rectal wall (arrowheads) at 7 to 8 o'clock without direct mural invasion. Compression and invasion could be difficult to distinguish on endoscopy.

## CONCLUSION

MRI is useful in assessing rectal submucosal tumours in terms of tumour localisation and characterisation and surgical planning. Radiologists should be familiar with the types and imaging and clinical features of different entities to facilitate accurate diagnosis and guide management.

## REFERENCES

1. Soh JS, Lee HS, Lee S, Bae J, Lee HJ, Park SH, et al. The clinical usefulness of endoscopic ultrasound-guided fine needle aspiration and biopsy for rectal and perirectal lesions. *Intest Res.* 2015;13:135-44. [crossref](#)
2. Ganeshan D, Bhosale P, Yang T, Kundra V. Imaging features of carcinoid tumors of the gastrointestinal tract. *AJR Am J Roentgenol.* 2013;201:773-86. [crossref](#)
3. Rodrigues A, Castro-Pocas F, Pedroto I. Neuroendocrine rectal tumors: main features and management. *GE Port J Gastroenterol.* 2015;22:213-20. [crossref](#)
4. Kim H, Kim JH, Lim JS, Choi JY, Chung YE, Park MS, et al. MRI findings of rectal submucosal tumors. *Korean J Radiol.* 2011;12:487-98. [crossref](#)
5. Bader TR, Semelka RC, Chiu VC, Armao DM, Woosley JT. MRI of carcinoid tumors: spectrum of appearances in the gastrointestinal tract and liver. *J Magn Reson Imaging.* 2001;14:261-9. [crossref](#)
6. Reznick RH. CT/MRI of neuroendocrine tumours. *Cancer Imaging.* 2006;6:S163-77. [crossref](#)
7. Lotfalizadeh E, Ronot M, Wagner M, Cros J, Couvelard A, Vullierme MP, et al. Prediction of pancreatic neuroendocrine tumor grade with MR imaging features: added value of diffusion-weighted imaging. *Eur Radiol.* 2017;27:1748-59. [crossref](#)
8. Kim M, Kang TW, Kim YK, Kim SH, Kwon W, Ha SY, et al. Pancreatic neuroendocrine tumour: correlation of apparent diffusion coefficient or WHO classification with recurrence-free survival. *Eur J Radiol.* 2016;85:680-7. [crossref](#)
9. Levy AD, Remotti HE, Thompson WM, Sobin LH, Miettinen M. Gastrointestinal stromal tumors: radiologic features with pathologic correlation. *Radiographics.* 2003;23:283-304. [crossref](#)
10. Yu MH, Lee JM, Baek JH, Han JK, Choi BI. MRI features of gastrointestinal stromal tumors. *AJR Am J Roentgenol.* 2014;203:980-91. [crossref](#)
11. van der Zwan SM, DeMatteo RP. Gastrointestinal stromal tumor: 5 years later. *Cancer.* 2005;104:1781-8. [crossref](#)
12. Kang JH, Kim SH, Kim YH, Rha SE, Hur BY, Han JK. CT features of colorectal schwannomas: differentiation from gastrointestinal stromal tumors. *PLoS One.* 2016;11:e0166377. [crossref](#)
13. van Schaik PM, Ernst MF, Meijer HA, Bosscha K. Melanoma of the rectum: a rare entity. *World J Gastroenterol.* 2008;14:1633-5. [crossref](#)
14. McLaughlin CC, Wu XC, Jemal A, Martin HJ, Roche LM, Chen VW. Incidence of noncutaneous melanomas in the U.S. *Cancer.* 2005;103:1000-7. [crossref](#)
15. Mason JK, Helwig EB. Ano-rectal melanoma. *Cancer.* 1966;19:39-50. [crossref](#)
16. Wong VK, Lubner MG, Menias CO, Mellnick VM, Kennedy TA, Bhalla S, et al. Clinical and imaging features of noncutaneous melanoma. *AJR Am J Roentgenol.* 2017;208:942-59. [crossref](#)
17. Matsuoka H, Nakamura A, Iwamoto K, Sugiyama M, Hachiya J, Atomi Y, et al. Anorectal malignant melanoma: preoperative usefulness of magnetic resonance imaging. *J Gastroenterol.* 2005;40:836-42. [crossref](#)
18. Kohli S, Narang S, Singhal A, Kumar V, Kaur O, Chandoke R. Malignant melanoma of the rectum. *J Clin Imaging Sci.* 2014;4:4. [crossref](#)
19. Falch C, Stojadinovic A, Hann-von-Weyhern C, Protic M, Nissan A, Faries MB, et al. Anorectal malignant melanoma: extensive 45-year review and proposal for a novel staging classification. *J Am Coll Surg.* 2013;217:324-35. [crossref](#)
20. Devojee M, Akarsh MP, Jagan Mohan Rao K. A case report of infiltrating ductal carcinoma of breast metastasizing to the rectum. *IOSR J Dent Med Sci.* 2015;14:1-3.
21. Mourra N, Jouret-Mourin A, Lazure T, Audard V, Albiges L, Malbois M, et al. Metastatic tumors to the colon and rectum: a multi-institutional study. *Arch Pathol Lab Med.* 2012;136:1397-401. [crossref](#)
22. Zheng G, Li H, Li J, Zhang X, Zhang Y, Wu X. Metastatic renal clear cell carcinoma to the rectum, lungs, ilium, and lymph nodes: a case report. *Medicine (Baltimore).* 2017;96:e5720. [crossref](#)
23. Del Frate C, Girometti R, Pittino M, Del Frate G, Bazzocchi M, Zuiani C. Deep retroperitoneal pelvic endometriosis: MR imaging appearance with laparoscopic correlation. *Radiographics.* 2006;26:1705-18. [crossref](#)
24. Yoon JH, Choi D, Jang KT, Kim CK, Kim H, Lee SJ, et al. Deep rectosigmoid endometriosis: "mushroom cap" sign on T2-weighted MR imaging. *Abdom Imaging.* 2010;35:726-31. [crossref](#)
25. Coutinho A Jr, Bittencourt LK, Pires CE, Junqueira F, Lima CM, Coutinho E, et al. MR imaging in deep pelvic endometriosis: a pictorial essay. *Radiographics.* 2011;31:549-67. [crossref](#)
26. Yang DM, Park CH, Jin W, Chang SK, Kim JE, Choi SJ, et al. Tailgut cyst: MRI evaluation. *AJR Am J Roentgenol.* 2005;184:1519-23. [crossref](#)
27. Aflalo-Hazan V, Rousset P, Mourra N, Lewin M, Azizi L, Hoeffel C. Tailgut cysts: MRI findings. *Eur Radiol.* 2008;18:2586-93. [crossref](#)
28. Dwarkasing RS, Verschuuren SI, van Leenders GJLH, Braun LMM, Krestin GP, Schouten WR. Primary cystic lesions of the retrorectal space: MRI evaluation and clinical assessment. *AJR Am J Roentgenol.* 2017;209:790-6. [crossref](#)
29. Saba L, Fellini F, Greco FG, Leonzio A, Cionci G, Consolo D, et al. MRI evaluation of not complicated Tailgut cyst: case report. *Int J Surg Case Rep.* 2014;5:761-4. [crossref](#)